Analysis of the variation in the determination of the shear modulus of the erythrocyte membrane: Effects of the constitutive law and membrane modeling

P. Dimitrakopoulos*

Department of Chemical and Biomolecular Engineering, University of Maryland, College Park, Maryland 20742, USA

(Received 18 February 2012; published 23 April 2012)

Despite research spanning several decades, the exact value of the shear modulus G_s of the erythrocyte membrane is still ambiguous, and a wealth of studies, using measurements based on micropipette aspirations, ektacytometry systems and other flow chambers, and optical tweezers, as well as application of several models, have found different average values in the range 2–10 μN/m. Our study shows that different methodologies have predicted the correct shear modulus for the specific membrane modeling employed, i.e., the variation in the shear modulus determination results from the specific membrane modeling. Available experimental findings from ektacytometry systems and optical tweezers suggest that the dynamics of the erythrocyte membrane is strain hardening at both moderate and large deformations. Thus the erythrocyte shear modulus cannot be determined accurately using strain-softening models (such as the neo-Hookean and Evans laws) or strain-softening/strain-hardening models (such as the Yeoh law), which overestimate the erythrocyte shear modulus. According to our analysis, the only available strain-hardening constitutive law, the Skalak *et al.* law, is able to match well both deformation-shear rate data from ektacytometry and force-extension data from optical tweezers at moderate and large strains, using an average value of the shear modulus of $G_s = 2.4$–2.75 μN/m, i.e., very close to that found in the linear regime of deformations via force-extension data from optical tweezers, $G_s = 2.5 \pm 0.4$ μN/m. In addition, our analysis suggests that a standard deviation in G_s of 0.4–0.5 μN/m (owing to the inherent differences between erythrocytes within a large population) describes well the findings from optical tweezers at small and large strains as well as from micropipette aspirations.

DOI: 10.1103/PhysRevE.85.041917 PACS number(s): 87.16.D−, 87.19.U−

I. INTRODUCTION

A human erythrocyte is essentially a capsule (i.e., a membrane-enclosed fluid volume) where the liquid interior (cytoplasm) is a concentrated hemoglobin solution that behaves as a Newtonian fluid with viscosity $\mu_c \approx 6$–10 m Pa s [1,2]. In healthy blood and in the absence of flow, the average human erythrocyte assumes a biconcave discoid shape of surface area $S_c = 135$ μm^2, with a diameter of 7.8 μm and a thickness varying from 0.8–2.6 μm at physiological osmolarity, resulting in a volume of $V_c = 94$ μm^3 [3,4]. The erythrocyte membrane is a complex multilayered object consisting of a 4-nm-thick lipid bilayer (which is essentially a two-dimensional incompressible fluid with no shear resistance) and an underlying elastic network of spectrin (which exhibits shear resistance like a two-dimensional elastic solid) [4].

Despite research spanning several decades, the exact value of the shear modulus G_s of the erythrocyte membrane is still ambiguous, and a wealth of studies, using measurements based on micropipette aspirations, ektacytometry systems and other flow chambers, and optical tweezers, as well as application of different models, have found different average values in the range 2–10 μN/m. Early experimental studies using micropipette aspiration reported an average shear modulus of $G_s = 4$–10 μN/m [5–7], while models proposed a strain-dependent shear modulus with a value near $G_s = 2$ μN/m at low strains; e.g., see Ref. [8]. In 1999, Hénon *et al.* [9], utilizing optical tweezers at small strains, found the membrane shear modulus to be $G_s = 2.5 \pm 0.4$ μN/m. Later studies, using force-extension data from optical tweezers and matching them with continuum and molecular models, found a shear modulus in the high range, $G_s = 8.3$ μN/m [10–12]. In our recent work [13], we compared our computational results with ektacytometry findings [14] and found a very good match for a shear modulus very close to the average value found by optical tweezers at low strains, $G_s = 2.5$ μN/m [9]. (To facilitate the subsequent discussion, in several places only the shear modulus value will be presented with the implicit assumption that its units are always μN/m.)

The significant discrepancies between these values suggest a need to examine the methodologies employed. Our review of published studies on the determination of the erythrocyte shear modulus reveals the following conclusions (as also discussed in Secs. III and IV). (i) Several studies are approximate since they utilize simple (or even crude) models and thus, at best, they find the order of magnitude of the shear modulus rather than its exact value. (ii) From the rest of the studies, which rely on accurate models, many utilize identical or very similar methodologies and thus it is not surprising that they predict a similar value for the shear modulus. Therefore, from the available large number of studies employing accurate models, only a much smaller set is truly independent. (iii) This small set of independent methodologies still predicts different values of the shear modulus. Thus a question naturally arises as to the reasons for this variation on the shear modulus determination.

Based on the above, the present paper has two main goals: (a) to explain why different methodologies predict different values of the erythrocyte shear modulus, and (b) to predict accurately the value of the shear modulus and, in particular, its average value and the range of its possible variation (owing to the inherent differences between erythrocytes within a large population).

*dimitrak@umd.edu

In Sec. II, we review several constitutive laws that have been used for the continuum description of the erythrocyte membrane since they are the basis to relate the available experimental measurements to the erythrocyte shear modulus. Based on the nature of these constitutive laws and their relationship, in Sec. III we discuss the determination of the shear modulus via four distinct methodologies: force-extension data from optical tweezers at small and large strains, deformation-shear rate data from ektacytometry, and data from micropipette aspirations. A review of additional methodologies on the shear modulus of the erythrocyte membrane has been included in Sec. IV.

We emphasize that our review of the existing studies on the determination of the erythrocyte shear modulus included in this paper cannot be all inclusive owing to the difficulty in finding all papers published and, most important, to the limited space commonly available for the references in a given publication. Thus, in this work, we include and discuss a few representative publications for several methodologies employed on shear modulus determination. Our comparisons and comments on earlier studies do not intend, by any means, to discount any previous study; all of them have provided invaluable information on the challenging problem of the physics of erythrocyte dynamics and its modeling.

II. MEMBRANE DYNAMICS

A. Common constitutive laws

Several constitutive laws have been used for the continuum description of thin elastic membranes such as that of the erythrocyte and many artificial capsules; see, e.g., [10,13,15–17]. These laws describe the principal elastic tensions τ_i $(i = 1,2)$ on the membrane as a function of the principal stretch ratios λ_i. Note that $\lambda_i = ds_i/dS_i$, where dS_i and ds_i denote line elements in the reference and the deformed shapes, while the principal strain components are given by $e_i = (\lambda_i^2 - 1)/2$ [15]. Below we present the elastic tension τ_1 for five constitutive laws; to calculate τ_2, reverse the λ_i subscripts.

The Hooke (H) law (physically valid for small deformations) assumes that the membrane tensions depend linearly on the surface strain [15],

$$\tau_1^{\mathrm{H}} = \frac{2G_s^{\mathrm{H}}}{1-\nu_s}(e_1 + \nu_s e_2) = \frac{G_s^{\mathrm{H}}}{1-\nu_s}\left[\lambda_1^2 - 1 + \nu_s\left(\lambda_2^2 - 1\right)\right], \tag{1}$$

where G_s^{H} is the shear modulus associated with this law and ν_s is the surface Poisson ratio ($\nu_s \neq 1$).

The neo-Hookean (NH) law, a special case of the Mooney-Rivlin law, results from the application of the corresponding three-dimensional law to a very thin membrane [15,18],

$$\tau_1^{\mathrm{NH}} = \frac{G_s^{\mathrm{NH}}}{\lambda_1\lambda_2}\left[\lambda_1^2 - \frac{1}{(\lambda_1\lambda_2)^2}\right], \tag{2}$$

where G_s^{NH} is the associated shear modulus. This law does not contain a parameter associated with area dilatation which is implicitly embodied into the law.

The Yeoh law (YE) [19] is a higher-order extension of the neo-Hookean law; its application to a very thin membrane gives the corresponding two-dimensional law [18],

$$\tau_1^{\mathrm{YE}} = \frac{G_s^{\mathrm{YE}}}{\lambda_1\lambda_2}\left[\lambda_1^2 - \frac{1}{(\lambda_1\lambda_2)^2}\right] \times\left\{1 + 2C_2^{\mathrm{YE}}\left[\lambda_1^2 + \lambda_2^2 + \frac{1}{(\lambda_1\lambda_2)^2} - 3\right] + 3C_3^{\mathrm{YE}}\left[\lambda_1^2 + \lambda_2^2 + \frac{1}{(\lambda_1\lambda_2)^2} - 3\right]^2\right\}, \tag{3}$$

where G_s^{YE} is the associated shear modulus, and C_2^{YE} and C_3^{YE} are dimensionless parameters.

The Skalak *et al.* (SK) law [20] adds nonlinearly the area dilatation to the shear deformation,

$$\tau_1^{\mathrm{SK}} = \frac{G_s^{\mathrm{SK}}}{\lambda_1\lambda_2}\left\{\lambda_1^2\left(\lambda_1^2 - 1\right) + C(\lambda_1\lambda_2)^2[(\lambda_1\lambda_2)^2 - 1]\right\}. \tag{4}$$

In the equation above, G_s^{SK} is the shear modulus associated with this law, while the dimensionless parameter C is associated with the area-dilatation modulus G_a^{SK} of the membrane (scaled with its shear modulus). In particular, analysis in the limit of small deformations shows that the area-dilatation modulus is $G_a^{\mathrm{SK}} = G_s^{\mathrm{SK}}(1 + 2C)$ [15].

The Evans (EV) law [17,21] adds linearly the area dilatation to the shear deformation,

$$\tau_1^{\mathrm{EV}} = G_s^{\mathrm{EV}}\left[\frac{\lambda_1^2 - \lambda_2^2}{2(\lambda_1\lambda_2)^2} + C^{\mathrm{EV}}(\lambda_1\lambda_2 - 1)\right], \tag{5}$$

where G_s^{EV} is the shear modulus associated with this law, while the dimensionless parameter C^{EV} represents the area-dilatation modulus of the membrane (scaled with its shear modulus). Note that this law is also called Evans-Skalak law in some papers (e.g., [18,22]), probably because it appeared later in the book of Evans and Skalak [23].

It is of interest to know that the Skalak *et al.* and Evans laws are two-dimensional laws, derived to represent thin elastic membranes. On the other hand, the (original) Hooke, neo-Hookean, and Yeoh laws are three-dimensional laws, derived to represent elastic materials. One may apply these laws to thin elastic membranes by either using the three-dimensional laws with a very small membrane thickness and volume incompressibility (i.e., $\lambda_1\lambda_2\lambda_3 = 1$) or utilizing the corresponding two-dimensional laws presented above. (The derivation of the two-dimensional laws from the original three-dimensional laws has been described in earlier papers; e.g., see Sec. 3.3 in Ref. [18] and Sec. 4.7 in Ref. [24].)

Under (mechanically) uniaxial extension or isotropic dilatation of capsules with finite surface area-dilatation resistance, it was found that the neo-Hookean and Evans laws are strain softening (i.e., their tensions increase sublinearly with the strain), while the Skalak *et al.* law is strain hardening (i.e., its tensions grow superlinearly with the strain) [15,18]. (Note that the linear increase used in these comparisons refers to the common slope of all laws in the linear regime of deformations.) The same behavior is observed in the steady-state dynamics of these capsules in planar extensional flows [25]. The behavior of the Yeoh law is more complicated; while at small deformations it behaves like the neo-Hookean law, due to the higher-order

correction included in the Yeoh law, its nature (strain softening or strain hardening) and its degree of strain softening vary with deformation at moderate and large deformations and depend on the particular choice of its two parameters, C_2^{YE} and C_3^{YE} [19].

B. Constitutive laws and local area incompressibility

Erythrocyte continuum models (such as the ones used to determine the membrane's shear modulus) commonly treat the erythrocyte membrane as a locally area-incompressible elastic solid by either employing a large area-dilatation modulus or imposing directly the local area-incompressibility constraint $\lambda_1\lambda_2 = 1$; see, e.g., [6,10,16].

By imposing locally the constraint $\lambda_1\lambda_2 = 1$, the constitutive laws described earlier are simplified to the following equations:

$$\tau_1^{\mathrm{H}} = \frac{G_s^{\mathrm{H}}}{1-\nu_s}\left(1-\frac{\nu_s}{\lambda_1^2}\right)\left(\lambda_1^2-1\right), \tag{6}$$

$$\tau_1^{\mathrm{NH}} = G_s^{\mathrm{NH}}\left(\lambda_1^2-1\right), \tag{7}$$

$$\tau_1^{\mathrm{YE}} = G_s^{\mathrm{YE}}\left(\lambda_1^2-1\right)\left[1+2C_2^{\mathrm{YE}}\left(\lambda_1^2+\frac{1}{\lambda_1^2}-2\right)+3C_3^{\mathrm{YE}}\left(\lambda_1^2+\frac{1}{\lambda_1^2}-2\right)^2\right], \tag{8}$$

$$\tau_1^{\mathrm{SK}} = G_s^{\mathrm{SK}}\lambda_1^2\left(\lambda_1^2-1\right), \tag{9}$$

$$\tau_1^{\mathrm{EV}} = G_s^{\mathrm{EV}}\frac{\lambda_1^2+1}{2\lambda_1^2}\left(\lambda_1^2-1\right). \tag{10}$$

It is interesting to note that several studies (e.g., [5,6,10,12,26]) referred to and/or employed the Evans law under local area incompressibility in the form

$$\tau_s^{\mathrm{EV}} = \frac{G_s^{\mathrm{EV}}}{2}\left(\lambda_1^2-\frac{1}{\lambda_1^2}\right), \quad \text{where} \quad \tau_s = \frac{\tau_1-\tau_2}{2}. \tag{11}$$

In Fig. 1, we plot the principal tension τ_1 (scaled with its associated shear modulus) as a function of the principal strain $e_1 = (\lambda_1^2-1)/2$ for all of the laws studied in this paper. Note that for the Hooke law, we used $\nu_s = 1/3$, which produces a practically linear tension-strain dependence up to $e_1 = 1.5$ (or $\lambda_1 = 2$) included in this figure, with a slope very close to the common slope of all laws at small deformations. For the Yeoh law, we used $C_2^{\mathrm{YE}} = 0$ and $C_3^{\mathrm{YE}} = 1/15$, i.e., the value of these two parameters (according to our notation and definition) employed in Ref. [10] to match erythrocyte's force-extension data from optical tweezers at large strains.

Figure 1 shows that even under local area incompressibility, the Skalak *et al*. law is strain hardening, the neo-Hookean and Evans laws are strain softening, while the Evans law is more strain softening than the neo-Hookean law. For the particular choice of the parameters C_2^{YE} and C_3^{YE}, after the initial strain-softening behavior at low deformations, the Yeoh law becomes strain hardening at large strains.

Small-deformation behavior. When local area incompressibility is enforced and the deformation is very small, i.e., $\lambda_1^2 = 1+\varepsilon$, where $|\varepsilon| \ll 1$, all aforementioned constitutive laws result in the same equation, i.e.,

$$\tau_1^{\alpha} = G_s^{\alpha}\,\varepsilon, \quad \text{where} \quad \alpha = \mathrm{H, NH, YE, SK, EV}, \tag{12}$$

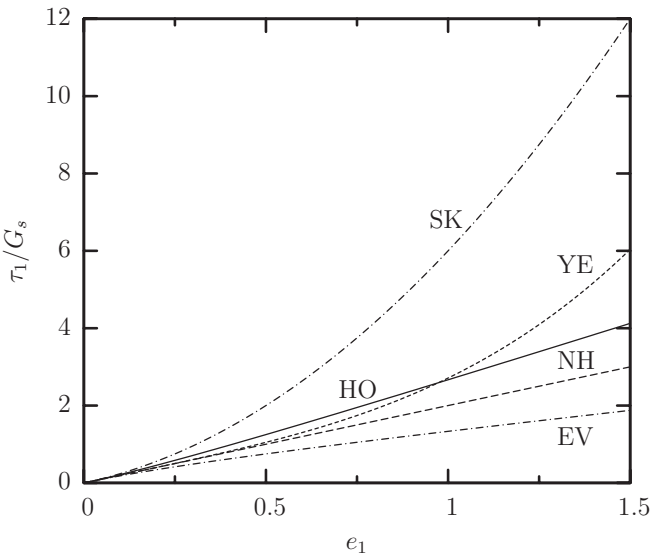

FIG. 1. Principal tension τ_1 (scaled with its associated shear modulus) as a function of the principal strain e_1 for the Hooke (HO), neo-Hookean (NH), Yeoh (YE), Skalak *et al*. (SK), and Evans (EV) laws under local area incompressibility, $\lambda_1\lambda_2 = 1$. For the Hooke law, we used $\nu_s = 1/3$, while for the Yeoh law, we used $C_2^{\mathrm{YE}} = 0$ and $C_3^{\mathrm{YE}} = 1/15$.

as simple perturbation algebra shows. Thus, under local area incompressibility and in the small-deformation regime, all laws produce identical tension-extension behavior for the same shear modulus, i.e.,

$$G_s^{\mathrm{H}} = G_s^{\mathrm{NH}} = G_s^{\mathrm{YE}} = G_s^{\mathrm{SK}} = G_s^{\mathrm{EV}}. \tag{13}$$

In essence, all constitutive laws behave as the Hooke law due to the linearization inherent in the regime of small deformations.

Non-small-deformation behavior. In moderate and large deformations, the different constitutive laws produce different behavior. Based on the strain-hardening or strain-softening nature of each law, we expect that for a given deformation, the more strain-softening law should produce the same tensions as a less strain-softening law, but for a higher shear modulus.

This behavior has been identified for the deformation of capsules with moderate area-dilatation resistance. For example, by matching the force-deformation curves derived from (mechanical) compression experiments, Carin *et al*. [27] showed that the strain-softening Evans law produces an almost 40% higher shear modulus than the Skalak *et al*. law [27].

In addition, if the matching is not valid over the entire deformation range, we expect the difference in the predicted shear moduli to increase with the deformation of matching. Thus, at small deformations, all laws predict the same shear modulus; by matching at moderate deformations, the more strain-softening law should predict a higher shear modulus, while by matching at large deformations, the more strain-softening law should predict a much higher shear modulus.

This was shown in Fig. 21(b) of our earlier work [25], where we plot the steady-state maximum principal tensions $\tau_{\max}^{P}$ as a function of the capsule extension/length L_c, for a neo-Hookean and a Skalak capsule with $C = 1$ in a planar extensional flow. (Note that in our earlier work, the tensions were scaled with the shear modulus of each law, while the capsule length was

scaled with its equilibrium length.) When $L_c = 1.5$ (extension 50%), matching the maximum tensions of these laws requires $G_s^{\mathrm{NH}}/G_s^{\mathrm{SK}} \approx 1.7$; the moduli ratio increases to $G_s^{\mathrm{NH}}/G_s^{\mathrm{SK}} \approx 2.5,3.4$ for lengths $L_c = 2,2.5$ (or extension 100%, 150%).

To estimate the difference in the predicted shear modulus of these constitutive laws under local area incompressibility, we match the local tensions given by each law for the same stretch ratio. Based on this, the following relationships are derived:

$$G_s^{\mathrm{NH}} = \lambda_1^2\, G_s^{\mathrm{SK}},\quad G_s^{\mathrm{EV}} = \frac{2\lambda_1^4}{\lambda_1^2+1}\, G_s^{\mathrm{SK}},\quad \text{and}$$
$$G_s^{\mathrm{YE}} = \frac{\lambda_1^2 G_s^{\mathrm{SK}}}{1+2C_2^{\mathrm{YE}}\left(\lambda_1^2+\frac{1}{\lambda_1^2}-2\right)+3C_3^{\mathrm{YE}}\left(\lambda_1^2+\frac{1}{\lambda_1^2}-2\right)^2}. \tag{14}$$

To derive an estimation of the relative magnitude for the shear modulus of these laws, we can approximate the stretch ratio λ_1 with the ratio of the extension of the deformed erythrocyte to its extension at the reference (i.e., equilibrium) shape which occurs in a given experimental system. For example, if we assume that at moderate deformations in ektacytometry systems or optical tweezers $\lambda_1^2 = 2$ (or $\lambda_1 \approx 1.41$), then the equations above predict

$$G_s^{\mathrm{NH}} \approx 2G_s^{\mathrm{SK}},\quad G_s^{\mathrm{EV}} \approx 2.67G_s^{\mathrm{SK}},\quad \text{and}$$
$$G_s^{\mathrm{YE}} \approx 1.90G_s^{\mathrm{SK}}. \tag{15}$$

At large deformations (such as in optical tweezer experiments at large strains), the erythrocyte axial diameter is increased to almost 100%; in this case, our prediction for $\lambda_1 = 2$ gives

$$G_s^{\mathrm{NH}} \approx 4G_s^{\mathrm{SK}},\ G_s^{\mathrm{EV}} \approx 6.4G_s^{\mathrm{SK}},\quad \text{and}$$
$$G_s^{\mathrm{YE}} \approx 1.99G_s^{\mathrm{SK}}. \tag{16}$$

The predictions above verify our earlier discussion in this section that for matching in a specific deformation range, the more strain-softening law should produce the same tensions as a less strain-softening law but for a higher shear modulus, while the difference in the predicted shear moduli should increase with the deformation range of matching.

In Fig. 2, we plot the shear modulus of the neo-Hookean, Yeoh, and Evans laws (scaled with the shear modulus of the Skalak *et al*. law) as a function of the stretch ratio λ_1. This figure shows clearly that owing to its strain hardening at large strains for the specific choice of the parameters C_2^{YE} and C_3^{YE}, the Yeoh law should produce a good match at large strains for membranes following the Skalak *et al*. law. It is of interest to note that for a stretch ratio λ_1 in the range [1.35,2] (which almost covers the extensions used in optical tweezer experiments at large strains [10]), the Yeoh's shear modulus is $G_s^{\mathrm{YE}} \approx 2G_s^{\mathrm{SK}}$ with an error of only $\pm 10\%$.

It is of interest to note that the shear resistance of the erythrocyte membrane results from its spectrin cytoskeleton, which may undergo local area changes under the constraint of fixed total area being enclosed beneath the lipid bilayer in the erythrocyte membrane [13,28,29]. In our present work, we utilize the assumption of local area incompressibility (so that we are able to determine the relationship between different constitutive laws) because this assumption has been employed by earlier shear modulus finding methodologies, e.g., via force-extension data from optical tweezers at moderate and large strains [10,11,30], via micropipette aspiration [6,7,26], and from electrically induced deformation experiments [16], as discussed in more detail in Secs. III and IV.

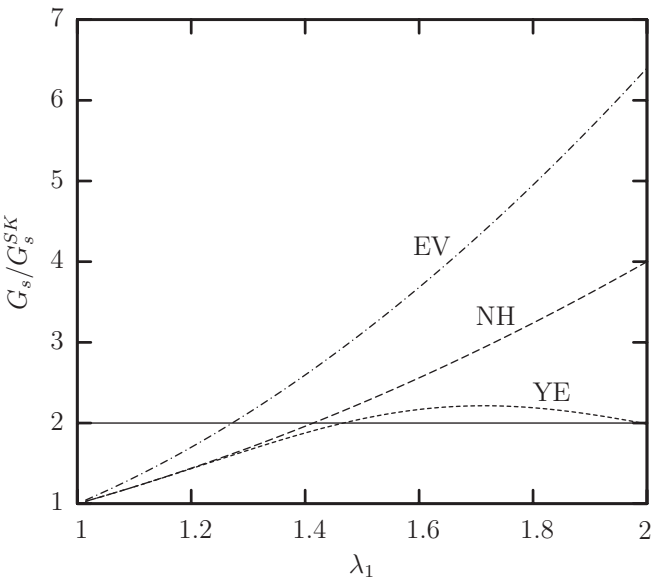

FIG. 2. Variation of the shear modulus of the neo-Hookean (NH), Yeoh (YE), and Evans (EV) laws [scaled with the shear modulus of Skalak *et al*. (SK) law] with the stretch ratio λ_1 so that all laws produce the same principal tension τ_1.

C. Finding the shear modulus of a membrane

In Sec. II B, we discussed that different constitutive laws should predict different estimations of the shear modulus of the erythrocyte membrane, depending on the degree of strain softening of each law and the deformation range of matching. Thus, a question naturally arises as to how to determine accurately the shear modulus of a given membrane and, in particular, of the erythrocyte. To help answer this question (which actually constitutes a research interest spanning several decades), two major statements can be made.

First, if the dynamics of a membrane is known to follow a given constitutive law in a range of deformations, then the shear modulus predicted by this law in this deformation range represents an accurate determination of the shear modulus of this membrane.

The statement above does not imply that if a constitutive law matches some experimental findings in a given range (e.g., the force-deformation curve from compression experiments, the deformation-shear rate curve from ektacytometry systems, or the force-extension relationship from optical tweezers at large strains), then this means that the dynamics of this membrane follows this law. Due to the bulk (and thus simplistic) nature of some experimental findings, these can be matched in a given range or even in the entire range of available deformations via one or several laws, without the membrane to follow one or any of these laws.

For example, obviously the biocompatible alginate capsule, used in the compression experiments of Carin *et al*. [27] mentioned earlier, cannot be at the same time strain hardening and strain softening since it was found that the strain-hardening Skalak *et al*. law as well as the strain-softening Evans law describe well the capsule's force-deformation compression curves. In reality, this capsule may follow one of these two laws or even none of them. Again this points to the simplistic nature of some available experimental findings.

Therefore, to find the constitutive law which truly describes the dynamics of a certain capsule (and thus its real shear modulus), more detailed (or complicated) experimental data are needed, i.e., using different experimental data (e.g., force-deformation but also deformation-shear rate data) and probably including information about local properties describing the capsule dynamics as opposed to the commonly available bulk-type experimental data (e.g., force-deformation or deformation-shear rate data).

For example, Lefebvre and Barthès-Biesel [31] proposed to flow capsules into a microchannel of comparable dimensions and observe local details of its interfacial shape as a function of the flow rate (including the curvature along the capsule profile) as a way to deduce the membrane shear modulus. Based on this, alginate capsules were found to show a strain-hardening dynamics best modeled by the Skalak *et al*. law with a small prestress.

The second major conclusion which can be drawn on this subject is that to avoid the complications arising from the fact that different laws predict different values of the membrane shear modulus, based on experimental findings at moderate and large deformations, one may consider the membrane dynamics at small deformations where all laws predict identical value of the shear modulus. Thus, the membrane moduli are formally defined by basic deformations in the linear regime of deformations. In particular, the (surface) Young modulus E_s (which is associated with the shear modulus G_s) is measured by the membrane response to a uniaxial extension, while the area-dilatation modulus G_a is measured by the membrane response to an isotropic tension [15,20].

The small-deformation regime offers an additional advantage to the shear-modulus finding methodologies, which employ an analytical equation to relate the membrane shear modulus with the experimental measurements; due to the linearization inherent in this deformation regime, the required relationship is, in general, easier to derive than in the (nonlinear) regime of large deformations.

III. NATURE AND SHEAR MODULUS OF THE ERYTHROCYTE MEMBRANE

Nature of erythrocyte membrane under strain. Measurements in ektacytometry systems have long shown that the erythrocyte's (ektacytometry) deformation increases logarithmically with the shear stress in both moderate and large deformations (see, for example, Fig. 3 in Ref. [14].) This finding reveals two conclusions: (a) the cell membrane has a single nature under both moderate and large strains, i.e., it is either strain hardening or strain softening, and (b) this single nature is strain hardening since the deformation-shear stress dependence is logarithmic. In addition, force-extension data from optical tweezers show clearly a hard-straining behavior at large strains, as has been identified in earlier studies; e.g., see Fig. 8 in Ref. [10]. The shear resistance of the erythrocyte membrane results from its elastic network of spectrin [4], while the strain-hardening nature of the spectrin cytoskeleton with deformation has also been identified via computational modeling [11,32].

Our reasoning based on the experimental findings suggests that the erythrocyte membrane is strain hardening for nonsmall deformations, i.e., for both moderate and large strains. In this case, the erythrocyte shear modulus cannot be determined accurately using strain-softening models (such as the neo-Hookean and Evans laws) or strain-softening/strain-hardening models (such as the Yeoh law). In particular, both types of laws are expected to produce a higher value of the shear modulus, as discussed in Sec. II B.

Determination of shear modulus at small strains via force-extension data from optical tweezers. In 1999, Hénon *et al*. [9], utilizing optical tweezers at small strains (stretching force <15 pN), determined the membrane shear modulus to be $G_s = 2.5 \pm 0.4$ μN/m. The discotic cell at rest was modeled by two parallel disks submitted to zero stress at their border. Owing to the linear regime of deformations, the early study employed constitutive laws from linear elasticity to relate the cell's transverse diameter with the applied force and the shear modulus.

To support their high value of the membrane shear modulus found by optical tweezers at large strains, Suresh and coworkers [10] discussed several possible reasons for the low shear modulus found by Hénon *et al*. [9], including "idealization of a biconcave cell as a two-dimensional planar disk" and "neglecting the effects of the relatively large contact region between the cell and the beads." In our opinion, these possible reasons do not constitute proofs, while so far no study has actually challenged the findings of Hénon *et al*. [9] at low strains, e.g., by proving that either the experiments or the employed analytical model are erroneous.

It is of interest to note that the earlier theoretical model of Fischer *et al*. [8] also suggested a low value of $G_s = 2$ μN/m at small strains to explain experiments on red cells whose membrane shear modulus has been increased by treatment with diamide. To match the higher value of the shear modulus at large strains known from micropipette aspiration studies, the authors proposed a strain-dependent shear modulus [8].

Determination of shear modulus at moderate strains via deformation-shear rate data from ektacytometry. In our recent work [13], we developed a cytoskeleton-based continuum erythrocyte algorithm based on the Skalak *et al*. law. In addition, we compared our computational results with the ektacytometry deformation-shear rate findings reported in Fig. 3 of Hardeman *et al*. [14]. Our computational results capture two important aspects of the relationship between cell deformation and capillary number (or wall shear stress): (i) the dependence is logarithmic for the employed range of shear rates, and (ii) while using a log scale for the capillary number, our method produces a slope consistent with experimental results (see Fig. 3 in our earlier paper [13].) In addition, for $G_s = 2.4$ μN/m, the experimental and computational curves coincide, suggesting that the sample used in the experimental measurement had a shear modulus very close to the average

value found by optical tweezers at low strains, $G_s = 2.5\,\mu$N/m [9].

We emphasize that additional comparisons of our computational results reported in Ref. [13] with ektacytometry findings from different studies show that the matching shear modulus falls inside the range for G_s valid for most red blood cells at low strains, i.e., 1.7–3.3 μN/m [9], and rather close to the average value. In particular, the ektacytometry's deformation-shear stress data, included in Table 1 of Wang *et al*. [33] from the laser-assisted optical rotational cell analyzer (LORCA) ektacytometer, correspond to a shear modulus of $G_s = 2.3$; the ektacytometry data for the control (i.e., normal erythrocytes), included in Fig. 1 of Alexy *et al*. [34], correspond to $G_s = 2$; while new ektacytometry data received from Hardeman [35] correspond to $G_s = 2.1$. Therefore, our four comparisons reveal an average value of the shear modulus of $G_s = 2.2$.

Note that our comparisons involve experimental findings via the LORCA ektacytometer, which works at the human body temperature of 37 °, and its measurements show negligible standard deviation. Since all the remaining methodologies discussed in this paper determine the shear modulus at room temperature (near 25 °), we can apply a temperature correction to our shear modulus determination. In their micropipette aspiration study, Waugh and Evans [6] reported a 9% decrease in the shear modulus from 24.8 ° to 35.3 ° in their Table 1; using this correction, our average value of the shear modulus becomes $G_s = 2.4$. The slightly higher value of $G_s = 2.64$ is obtained if we use the 20% decrease from 25 ° to 35 ° reported in Fig. 11 in the electrically induced deformation methodology of Engelhardt and Sackmann [16].

Determination of shear modulus at moderate and large strains via force-extension data from optical tweezers. In a series of papers, Suresh and coworkers determined the shear modulus of the erythrocyte membrane by matching computational results from continuum and molecular models with their optical tweezer force-extension data at moderate and large strains (stretching force 20 to 198 pN); see, e.g., [10–12]. The results based on their continuum modeling were summarized in Ref. [10]. In particular, the authors utilized a finite-element program to solve for the cell shape deforming as in the optical tweezer experiments, assuming that the erythrocyte membrane follows either the neo-Hookean law (with or without enforcing local area incompressibility) or the Yeoh law (without enforcing local area incompressibility). During the deformation, the flow inside the erythrocyte was not considered; the cytoplasm was treated as an inviscid fluid, which acts to keep the interior volume constant. (Similar continuum modeling was employed in later studies from other groups with similar predictions; e.g., [36].)

As reported in Fig. 7 of the earlier study [10], the neo-Hookean law is able to describe adequately the cell's axial diameter at moderate strains only (stretching force 20 to 88 pN), but fails at higher strains since it cannot describe the erythrocyte's hard-straining behavior in this range of deformations. Without enforcing local area incompressibility, the shear modulus was found to vary in the range [5.3,11.3] due to the variation in the experimental data, with an average value of $G_s^{\mathrm{NH}} = 7.3$. The shear modulus under local area incompressibility is 75% of that without, i.e., it varies in the range [4,8.5] with an average value of $G_s^{\mathrm{NH}} = 5.5$ [10].

According to our estimation discussed in Sec. II B, the corresponding shear modulus for a membrane following the Skalak *et al*. law is expected to be about half that of the neo-Hookean law, i.e., under local area incompressibility it is expected to vary in the range [2,4.25] with an average value of $G_s^{\mathrm{SK}} = 2.75$. This is very close to that found in the linear regime of deformations, i.e., average value $G_s = 2.5$ and range [1.7,3.3] [9].

When the Yeoh law was used to described the erythrocyte membrane, the computations of Suresh and coworkers were able to describe adequately the cell's axial diameter at both moderate and large strains (stretching force 20 to 198 pN), as seen in Fig. 8 of the earlier study [10], due to the hard-straining nature of the Yeoh law at large strains (as also shown in our Fig. 1). Without enforcing local area incompressibility, they found the same range and average value as for their neo-Hookean law at moderate strains. (We note that the model was unable to match the transverse diameter; an optical matching for the average value of the experimental data suggests an average value for the shear modulus below 3.)

By using the shear modulus of the Yeoh law which best matches the erythrocyte axial diameter, and converting it to the corresponding shear modulus under local area incompressibility by multiplying with 0.75, as suggested by the authors (see Ref. [10] and Table 1 in Ref. [12]), we obtain the same values as for the neo-Hookean law. As shown clearly in our Fig. 2, for almost the entire range of the strains used in the work of Suresh and coworkers, the Yeoh's shear modulus is $G_s^{\mathrm{YE}} \approx 2G_s^{\mathrm{SK}}$ with an error of only $\pm 10\%$. Thus, again we obtain the same determination for the shear modulus of the Skalak *et al*. law: range [2,4.25] and average value of $G_s^{\mathrm{SK}} = 2.75$.

It is of interest to note that the recent study of Le *et al*. [36], which considered the same membrane modeling with that of Suresh and coworkers [10] but also solved the inner viscous flow utilizing their implicit immersed boundary method, reported a shear modulus range of [4.8,10] and an average value of $G_s^{\mathrm{YE}} = 7.3$, based on matching with the optical tweezer data for the axial diameter as shown in their Fig. 13. If we account for the missing local area incompressibility (by multiplying by 0.75) and convert to the Skalak *et al*. law (by dividing by 2), we get the range [1.8,3.75] which is very close to the range [1.7,3.3] found in the linear regime [9].

Therefore, the Skalak *et al*. law is the only employed law which is able to match well both deformation-shear rate data from ektacytometry and force-extension data from optical tweezers at moderate and large strains using a value of the shear modulus very close to that found in the linear regime of deformations, i.e., $G_s = 2.5\ \mu$N/m [9]. This reinforces further our earlier conclusion that the nature of the erythrocyte membrane is strain hardening at both moderate and large deformations.

An important conclusion here is that the shear modulus found by matching a constitutive law with experimental data in a specific range of deformations is not necessarily the same as that found in the linear regime of deformations, i.e., the true shear modulus of the membrane. For example, if the erythrocyte membrane follows the Skalak *et al*. law, then our understanding is that Suresh and coworkers [10–12] as well as other groups [36] found the shear modulus that represents

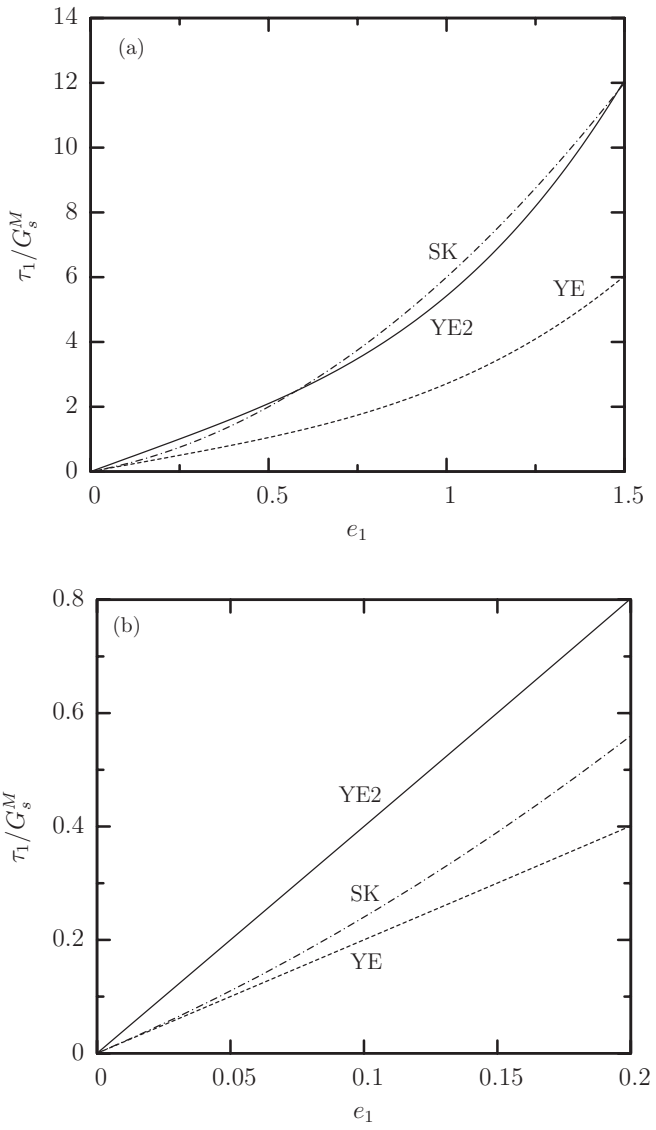

FIG. 3. Principal tension τ_1 (scaled with the membrane's shear modulus G_s^{M}) as a function of the principal strain e_1 for the Yeoh (YE) and the Skalak *et al.* (SK) laws having the membrane's shear modulus, i.e., $G_s^{\mathrm{YE}} = G_s^{\mathrm{SK}} = G_s^{\mathrm{M}}$. Also plotted is the tension-strain dependence YE2 for the Yeoh law having a shear modulus twice that of the membrane, $G_s^{\mathrm{YE}} = 2\,G_s^{\mathrm{M}}$. (a) Curve YE2 appears to match adequately the SK curve in moderate and large strains, while optically it also appears to produce a good matching at small strains owing to the large x-axis scale. (b) Working in the linear regime (e.g., plotting the data only for small strains), it is obvious that curve YE2 cannot match the common slope (i.e., the membrane's shear modulus G_s^{M}) of the other two curves.

the Yeoh law at large strains but not the true shear modulus of the erythrocyte membrane, as shown optically in Fig. 3 and explained in its caption.

Determination of shear modulus from micropipette aspiration. Different research groups have long used micropipette aspiration experiments to determine the mechanical properties of the erythrocyte membrane; see, e.g., [5–7,26,37]. These studies utilized the incompressible Evans law, given by Eq. (11), and an analytical equation to relate the pipette suction pressure with the aspiration length. Based on this methodology, the shear modulus was found to vary in the range 4–10 with a typical value of $G_s = 6$–7 at room temperature [5].

Hénon *et al.* [9] discussed several possible reasons to explain the difference between their low shear modulus value at the linear regime and the high value from the micropipette aspiration. According to their summary, "the shear modulus is expected to increase from the small to the finite deformation regime, and because the elastic modulus measured with micropipettes is a combination of the shear modulus and area compressibility [9]."

Our analysis suggests that this difference results from the constitutive law employed in the micropipette aspiration studies. Based on our discussion in Sec. II B, the Evans incompressible law should overestimate the erythrocyte shear modulus (based on the Skalak *et al.* law) by a factor of 2–3 at moderate deformations and much more at larger deformations. To show further the correspondence between the two laws, in the Appendix we employ Evans analysis for the statics of the micropipette aspiration, but utilize the incompressible Skalak *et al.* law, and show that the moduli ratio $G_s^{\mathrm{EV}}/G_s^{\mathrm{SK}}$ should vary in the range [1.5,3.6] for the aspiration lengths usually employed in the micropipette studies. Thus the typical value of $G_s = 6.5$ found by micropipette aspirations corresponds to a moduli ratio of $G_s^{\mathrm{EV}}/G_s^{\mathrm{SK}} = 6.5/2.5 = 2.6$, which is rather well representative of the overestimation of the Evans law (with respect to the Skalak *et al.* law) in these experiments.

It is of interest to note that the values of the standard deviation found in micropipette aspiration studies are consistent with the standard deviation of 0.4 found by Hénon *et al.* [9], if we scale them with the corresponding moduli ratio. For example, Waugh and Evans found $G_s = 6.61 \pm 1.24$; scaling this standard deviation with 2.5/6.61, we obtain 0.47. We also obtain the same scaled standard deviation from the study of Evans *et al.* [26], who found $G_s = 9 \pm 1.7$. Lelièvre *et al.* [37] found $G_s = 4.5 \pm 0.8$, and thus their scaled standard deviation is 0.44.

In essence, we believe that the (very) strain-softening Evans law cannot represent well the strain-hardening behavior of the erythrocyte membrane at nonlinear deformations, and thus methodologies which employ this law should always overestimate the shear modulus of the erythrocyte membrane.

IV. REVIEW OF ADDITIONAL METHODOLOGIES ON THE SHEAR MODULUS OF THE ERYTHROCYTE MEMBRANE

Cytoskeleton molecular models. A series of papers utilized spectrin-based molecular algorithms and compared their results with force-extension measurements via optical tweezers at moderate and large strains; see, e.g., [11,12,38]. These studies are based on the molecular algorithm of Suresh and coworkers, and thus it is not surprising that they predicted a shear modulus in the high range, $G_s = 8.3\ \mu$N/m [11,12,38], since this spectrin algorithm employs specific values for the associated molecular parameters that match the Yeoh continuum law, as discussed in Ref. [12]. Further, the shear modulus of the molecular algorithms originally results from the particular choice of the employed molecular parameters and not via matching with optical

tweezer measurements that is used only for verification (see Sec. 2.4 in Ref. [12] and Sec. 4.3 in Ref. [38]).

It is of interest to note that the molecular algorithms of Suresh and coworkers [11,12] and Hartmann [38], which do not account for the local area-incompressibility forces of the lipid bilayer, produce a practically linear force-extension relationship which does not match well the hard-straining nature of the erythrocyte shown in the experimental measurements (e.g., see Fig. 8 in Ref. [12] and Fig. 7 in Ref. [38]). By incorporating the constraint of local area incompressibility in the spectrin description, Karniadakis and coworkers [30] produced a very good match with the hard-straining force dependence for the axial diameter of the erythrocyte.

As discussed in our cytoskeleton-based continuum erythrocyte algorithm [13], the local area-incompressibility forces (i.e., locally isotropic forces) of the lipid bilayer should be accounted for in any spectrin modeling either continuum or molecular. However, in our opinion, enforcing a local area incompressibility on the spectrin membrane appears to be stricter than necessary, since the cytoskeleton can undergo local area changes under the constraint of fixed total area being enclosed beneath the lipid bilayer in the erythrocyte membrane [13,28,29]. (The main issue here is that the local area-incompressibility forces of the lipid bilayer produce incompressibility of the local area on the lipid bilayer, but not necessarily on the spectrin cytoskeleton.)

The incorporation of the local area-incompressibility constraint in the spectrin description [30] reduced the predicted shear modulus from $G_s = 8.3$ to $G_s = 6.3$. This reduction is in agreement with the correction factor of 0.75 suggested in the earlier studies of Suresh and coworkers [10,11] since $8.3 \times 0.75 = 6.2$, i.e., in essence the methodology of Karniadakis and coworkers [30], corresponds to an incompressible Yeoh law. Therefore, based on the analysis of this paper, if the parameters of Karniadakis' methodology are modified to match the Skalak *et al*. law, then we expect the prediction of the shear modulus to be within the range found by Hénon *et al*. [9].

Low-viscosity ektacytometry. Alternative ektacytometry systems have been developed by Wen and coworkers [39,40] that involve erythrocytes in the "wheel" orientation in low-viscosity surrounding liquids at moderate shear rates. Based on a simple analytical model (which assumes that the incompressible Evans law applies to the maximum elongation of the cell), the authors predicted a shear modulus of $G_s = 6.1$ via measurements through changes in laser-diffraction patterns, and a shear modulus of $G_s = 4.3$ via direct observations of erythrocyte deformation in a flow chamber.

Recently, MacMeccan *et al*. [41], utilizing a coupled lattice-Boltzmann/finite-element method, found good agreement with the experimental data on deformation versus flow rate in the flow chamber [39,40]. The numerical method utilizes the physiological conditions of the human erythrocyte with $G_s = 5.7$, but it does not enforce local area incompressibility. Observation of their Fig. 12 shows that a (computational) line with a smaller slope (i.e., a smaller G_s) matches better the experimental results, while the shear modulus is further reduced (by a factor of 0.75) if we enforce the local area-incompressibility constraint.

However, the experimental work of Wen and coworkers [39,40] used red blood cells from rabbits, which are smaller than human erythrocytes (i.e., mean diameter 6.5 μm) and thus probably have different properties, including equilibrium shape, inner viscosity, and shear modulus, while the effects of osmotic pressure and temperature are unclear for these cells. Until these issues are clarified, further discussion on these experimental measurements seems redundant.

Methodologies based on electrically induced deformation experiments. Engelhardt and Sackmann [16] developed a method to measure the shear modulus of the erythrocyte membrane based on the fixation and transient deformation of cells in a high-frequency electric field. The cell were subjected to both moderate and large deformations, while the shear modulus determination was based on moderate deformations (i.e., elongations less then 3 μm). Owing to the nonlinear deformations, the authors had to utilize an approximate sphere-to-ellipsoid deformation model that appears to be accurate at moderate deformations based on numerical tests via finite elements that the authors performed [16]. In addition, Engelhardt and Sackmann employed the incompressible Evans law and found an average value of the shear modulus of all cells of $G_s = 6.1$. Our analysis in Sec. II B suggests that the incompressible Evans law should overestimate the erythrocyte shear modulus based on the Skalak *et al*. law by a factor of 2–3 at moderate deformations. Thus their shear modulus corresponds to a Skalak *et al*. shear modulus of about $G_s^{\mathrm{SK}} = 6.1/2.5 = 2.44$, which is in excellent agreement with that found in the linear regime [9].

Additional methods. Korin *et al*. [22] utilized observations of erythrocytes flowing in microchannels at moderate deformations (relative cell extensions between 10% and 60%) and determined a shear modulus of $G_s = 3.7$. However, the earlier study used the incompressible Evans law which, based on our discussion in Sec. II B, should overestimate the erythrocyte shear modulus based on the Skalak *et al*. law by a factor of 2–3 at these deformations. Most important, to solve the flow dynamics, the Keller and Skalak model was employed, which is an approximate model that predicts only qualitatively the erythrocyte motion [42]. A major source of error in this model results from the omission of the shape-memory effects owing to the nonspherical quiescent erythrocyte shape; this is a phenomenon which has been identified only recently [43,44]. Thus, the Keller and Skalak model predicts with a small error the erythrocyte inclination, but overpredicts by a factor of 5–6 its tank-treading frequency [45], which is used in the model of Korin *et al*. [22] to determine the membrane shear modulus.

Therefore, the theoretical model of Korin *et al*. [22] is very approximate and the fact that its prediction of $G_s = 3.7$ appears to be realistic is because the model contains counterbalanced approximations, i.e., combined significant overprediction with significant underprediction of the true erythrocyte dynamics.

V. CONCLUSIONS

Despite research spanning several decades, the exact value of the shear modulus G_s of the erythrocyte membrane is still

ambiguous, and a wealth of studies, using measurements based on micropipette aspirations, ektacytometry systems and other flow chambers, and optical tweezers, as well as application of different models, have found different average values in the range 2–10 μN/m.

Our work shows that different methodologies have predicted the correct shear modulus for the specific membrane modeling employed, i.e., the variation in the shear modulus determination results from the specific membrane modeling. Available experimental findings from ektacytometry systems and optical tweezers suggest that the dynamics of the erythrocyte membrane is strain hardening at both moderate and large deformations. Thus the erythrocyte shear modulus cannot be determined accurately using strain-softening models (such as the neo-Hookean and Evans laws) or strain-softening/strain-hardening models (such as the Yeoh law), which overestimate the erythrocyte shear modulus. According to our analysis, the only available strain-hardening constitutive law, the Skalak *et al*. law, is able to match well both deformation-shear rate data from ektacytometry and force-extension data from optical tweezers at moderate and large strains, using a value of the shear modulus of $G_s = 2.4$–2.75 μN/m, i.e., very close to that found in the linear regime of deformations via force-extension data from optical tweezers, $G_s = 2.5 \pm 0.4$ μN/m [9]. Finally, our work suggests that this is the accurate value of the erythrocyte shear modulus and does not vary with strain. The range of the shear modulus variation (owing to the inherent differences between erythrocytes within a large population) appears to be well described with that found by Hénon *et al*. [9]; in particular, our analysis suggests that a standard deviation in G_s of 0.4–0.5 μN/m describes well the findings from optical tweezers at small and large strains as well as from micropipette aspirations.

We emphasize that the strain-hardening nature and the true value of the shear modulus are necessary for the understanding of experimental findings on erythrocytes dynamics (e.g., [8,14]), including their circulation in the blood system. In addition, the shear modulus is used in the determination of other properties of the erythrocyte membrane, such as its bending resistance and surface viscosity [8,17,26,30]. Thus we believe that it may be necessary to reconsider the determination of the bending modulus and the viscosity of the erythrocyte membrane from earlier studies, which utilized strain-softening models and high values for the shear modulus.

To improve the understanding of the erythrocyte dynamics, it would be very useful if experimental groups provide non-bulk-type data on erythrocyte deformation, such as local details of the interfacial shape of individual cells in basic flows (e.g., simple shear flow or planar extensional flow) or in confined solid geometries (e.g., microfluidic channels). In this case, the experimental studies should also provide information on the properties of the individual cells studied, including equilibrium shape and cytoplasm viscosity.

ACKNOWLEDGMENTS

This work was supported in part by the National Science Foundation and the National Institutes of Health.

APPENDIX: MICROPIPETTE ASPIRATION ANALYSIS BASED ON THE SKALAK *ET AL.* LAW

In this Appendix, we employ Evans analysis for the statics of the micropipette aspiration [46], but utilize the Skalak *et al*. law instead of the Evans law so that we can determine the shear modulus G_s^{SK} of the Skalak *et al*. law applicable to micropipette analysis.

As discussed in pages 122–124 in the work of Waugh and Evans [6], the principal stretch ratio along the meridian direction at a point outside the pipette entrance is given by

$$\lambda_1^2 = 1 + \left(\frac{R_p}{r}\right)^2 \left(\frac{2L_p}{R_p} - 1\right), \tag{A1}$$

where R_p is the pipette internal radius and L_p is the aspiration length. The pipette suction pressure is determined by integrating in the plane of the membrane from the pipette tip outward,

$$\Delta P = \frac{4}{R_p} \int_{R_p}^{\infty} \frac{\tau_s}{r} dr, \tag{A2}$$

where $\tau_s = (\tau_1 - \tau_2)/2$. Utilizing the incompressible Evans law for the principal tensions τ_1 and τ_2 and thus for τ_s given by Eq. (11), the authors found the pipette suction pressure to be

$$\Delta P = \left(\frac{G_s^{\mathrm{EV}}}{R_p}\right) \left[\left(\frac{2L_p}{R_p} - 1\right) + \ln\left(\frac{2L_p}{R_p}\right)\right]. \tag{A3}$$

(Note that the same result for ΔP was also found by Chien *et al*. [7], who applied the Evans law but considered the statics inside the pipette using a spherical cap model.)

Following the same analysis but for the incompressible Skalak *et al*. law, given by Eq. (9), we can easily show that

$$\tau_s^{\mathrm{SK}} = \frac{G_s^{\mathrm{SK}}}{2} \left(\lambda_1^2 - \frac{1}{\lambda_1^2}\right) \left(\lambda_1^2 + \frac{1}{\lambda_1^2} - 1\right), \tag{A4}$$

while the pipette suction pressure is now given by

$$\Delta P = \left(\frac{G_s^{\mathrm{SK}}}{R_p}\right) \left(\frac{2L_p}{R_p} - 1\right) \left(\frac{L_p}{R_p} + \frac{R_p}{2L_p} + \frac{1}{2}\right). \tag{A5}$$

Combining Eqs. (A3) and (A5), we find the moduli ratio for the two laws,

$$\frac{G_s^{\mathrm{EV}}}{G_s^{\mathrm{SK}}} = \frac{\left(\frac{2L_p}{R_p} - 1\right)\left(\frac{L_p}{R_p} + \frac{R_p}{2L_p} + \frac{1}{2}\right)}{\left(\frac{2L_p}{R_p} - 1\right) + \ln\left(\frac{2L_p}{R_p}\right)}. \tag{A6}$$

Different micropipette aspiration studies have utilized aspiration lengths of about $L_p/R_p = 1.5$–4; e.g., see [6,7,26,37]. In this range of L_p/R_p, the moduli ratio $G_s^{\mathrm{EV}}/G_s^{\mathrm{SK}}$ increases practically linearly with the aspiration length and takes on values of 1.5–3.6. Thus, even based on Evans micropipette analysis, if one uses Evans law to describe the tensions of a strain-hardening membrane following the Skalak *et al*. law, then this will result in a significant overestimation of the shear modulus.

It is of interest to note that Lelièvre *et al*. [37] reported that they used the Skalak *et al*. law and the Evans analysis in their micropipette aspiration study. However, Lelièvre *et al*. neglected the last factor for τ_s^{SK} shown in our Eq. (A4) and thus

found τ_s for the Evans law given by our Eq. (11) while they used the pipette suction pressure valid for the Evans law, i.e., Eq. (A3) above. [See Eqs. (4) and (5) in the earlier study [37].] We note that the factor $(\lambda_1^2 + \lambda_1^{-2} - 1)$ cannot be neglected in the nonlinear regime of deformations such as those used in the micropipette systems. Thus, in essence, Lelièvre *et al.* [37] utilized the Evans law with Evans micropipette analysis similarly to earlier studies; see, e.g., [6,46].

[1] R. Skalak, N. Özkaya, and T. C. Skalak, Annu. Rev. Fluid Mech. **21**, 167 (1989).
[2] N. Mohandas and J. A. Chasis, Sem. Hem. **30**, 171 (1993).
[3] E. A. Evans and Y.-C. Fung, Microvasc. Res. **4**, 335 (1972).
[4] O. K. Baskurt and H. J. Meiselman, Sem. Thromb. Hem. **29**, 435 (2003).
[5] R. M. Hochmuth and R. E. Waugh, Annu. Rev. Phys. **49**, 209 (1987).
[6] R. Waugh and E. A. Evans, Biophys. J. **26**, 115 (1979).
[7] S. Chien, K.-L. P. Sung, R. Skalak, S. Usami, and A. Tözeren, Biophys. J. **24**, 463 (1978).
[8] T. M. Fischer, C. W. M. Haest, M. Stöhr-Liesen, H. Schmid-Schönbein, and R. Skalak, Biophys. J. **34**, 409 (1981).
[9] S. Hénon, G. Lenormand, A. Richert, and F. Gallet, Biophys. J. **76**, 1145 (1999).
[10] J. P. Mills, L. Qie, M. Dao, C. T. Lim, and S. Suresh, Mech. Chem. Biosyst. **1**, 169 (2004).
[11] J. Li, M. Dao, C. T. Lim, and S. Suresh, Biophys. J. **88**, 3707 (2005).
[12] M. Dao, J. Li, and S. Suresh, Mater. Sci. Eng. C **26**, 1232 (2006).
[13] W. R. Dodson III and P. Dimitrakopoulos, Biophys. J. **99**, 2906 (2010).
[14] M. R. Hardeman, P. T. Goedhart, J. G. G. Dobbe, and K. P. Lettinga, Clin. Hemorheol. **14**, 605 (1994).
[15] D. Barthès-Biesel, A. Diaz, and E. Dhenin, J. Fluid Mech. **460**, 211 (2002).
[16] H. Engelhardt and E. Sackmann, Biophys. J. **54**, 495 (1988).
[17] E. A. Evans and R. M. Hochmuth, Biophys. J. **16**, 1 (1976).
[18] M. Rachik, D. Barthès-Biesel, M. Carin, and F. Edwards-Levy, J. Colloid Interface Sci. **301**, 217 (2006).
[19] O. H. Yeoh, Rubber Chem. Technol. **66**, 754 (1993).
[20] R. Skalak, A. Tözeren, R. P. Zarda, and S. Chien, Biophys. J. **13**, 245 (1973).
[21] E. A. Evans, Biophys. J. **13**, 926 (1973).
[22] N. Korin, A. Bransky, and U. Dinnar, J. Biomech. **40**, 2088 (2007).
[23] E. A. Evans and R. Skalak, *Mechanics and Thermodynamics of Biomembranes* (CRC, Boca Raton, FL, 1980).
[24] C. Pozrikidis, J. Comp. Phys. **169**, 250 (2001).
[25] W. R. Dodson III and P. Dimitrakopoulos, J. Fluid Mech. **641**, 263 (2009).
[26] E. Evans, N. Mohandas, and A. Leung, J. Clin. Invest. **73**, 447 (1984).
[27] M. Carin, D. Barthès-Biesel, F. Edwards-Lévy, C. Postel, and D. C. Andrei, Biotech. Bioeng. **82**, 207 (2003).
[28] T. M. Fischer, Biophys. J. **61**, 298 (1992).
[29] D. E. Discher, N. Mohandas, and E. A. Evans, Science **266**, 1032 (1994).
[30] D. A. Fedosov, B. Caswell, and G. E. Karniadakis, Biophys. J. **98**, 2215 (2010).
[31] Y. Lefebvre and D. Barthès-Biesel, J. Fluid Mech. **589**, 1570 (2007).
[32] R. Mukhopadhyay, H. W. G. Lim, and M. Wortis, Biophys. J. **82**, 1756 (2002).
[33] X. Wang, H. Zhao, F. Y. Zhuang, and J. F. Stoltz, Clin. Hemorheol. Microcirc. **21**, 291 (1999).
[34] T. Alexy, N. Nemeth, R. B. Wenby, R. M. Bauersachs, O. K. Baskurt, and H. J. Meiselman, Biorheology **44**, 361 (2007).
[35] M. R. Hardeman (private communication).
[36] D. V. Le, J. White, J. Peraire, K. M. Lim, and B. C. Khoo, J. Comp. Phys. **228**, 8427 (2010).
[37] J. C. Lelièvre, C. Bucherer, S. Geiger, C. Lacombe, and V. Vereycken, J. Phys. III (France) **5**, 1689 (1995).
[38] D. Hartmann, Biomech. Model Mechanobiol. **9**, 1 (2010).
[39] W. Yao, Z. Wen, Z. Yan, D. Sun, W. Ka, L. Xie, and S. Chien, J. Biomech. **34**, 1501 (2001).
[40] X. Liu, Z. Tang, Z. Zeng, X. Chen, W. Yao, Z. Yan, Y. Shi, H. Shan, D. Sun, D. He, and Z. Wen, Math. Biosci. **209**, 190 (2007).
[41] R. M. MacMeccan, J. R. Clausen, G. P. Neitzel, and C. K. Aidun, J. Fluid Mech. **618**, 13 (2009).
[42] S. R. Keller and R. Skalak, J. Fluid Mech. **120**, 27 (1982).
[43] M. Abkarian, M. Faivre, and A. Viallat, Phys. Rev. Lett. **98**, 188302 (2007).
[44] J. M. Skotheim and T. W. Secomb, Phys. Rev. Lett. **98**, 078301 (2007).
[45] W. R. Dodson III and P. Dimitrakopoulos, Phys. Rev. E **84**, 011913 (2011).
[46] E. A. Evans, Biophys. J. **13**, 941 (1973).